ACS OMEGA

Open Access

http://pubs.acs.org/journal/acsodf

Article

Bioassay-Guided Isolation and Identification of Cytotoxic Compounds from *Melaleuca quinquenervia* Fruits

Achara Raksat, Md Samiul Huq Atanu, Sheyanne Mendez, Rafael de la Zerda, Rui Sun, Sarot Cheenpracha, Marisa Wall, Charles J. Simmons, Philip G. Williams, Ghee T. Tan, Supakit Wongwiwatthananukit, and Leng Chee Chang*

Cite This: *ACS Omega* 2024, 9, 18516−18525

Read Online

ACCESS | Metrics & More | Article Recommendations | Supporting Information

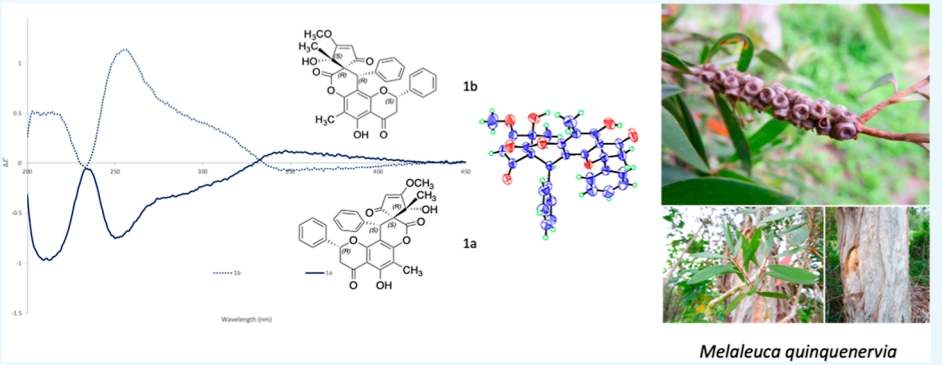

ABSTRACT: The fruit extract of *Melaleuca quinquenervia* yielded a total of 19 compounds, including two novel spiro-biflavonoid enantiomers (**1a** and **1b**) and a chalcone derivative (**3**). Their structures were determined through spectroscopic analysis. The enantiomers of the racemic mixture of compound **1** were successfully resolved into (+)-**1** and (−)-**1** using chiral-phase HPLC. Single-crystal X-ray diffraction analysis was also used to confirm the structure of **1**. The enantiomeric configurations of **1** and **2** were determined through a comparison of the calculated and experimental electronic circular dichroism spectra. Compounds **2** (melanervin), **14** (methyl betulinate), **15** (3-*O*-acetylbetulinic acid), and **16** (pyracrenic acid) were found to be highly cytotoxic, with compound **16** showing superior growth inhibition of nonsmall cell lung cancer cells (A549 cells) (IC_{50} 2.8 ± 0.1 μM) compared to cisplatin (IC_{50} 3.3 ± 0.0 μM), a positive control chemotherapeutic drug. Both compound **16** and cisplatin were significantly more cytotoxic toward A549 lung cancer cells compared to nontumorigenic Vero E6 cells.

1. INTRODUCTION

Melaleuca is a large evergreen tree that belongs to the Myrtaceae family and has around 280 species distributed across eastern Australia, Papua New Guinea, and New Caledonia.[1] *Melaleuca leucadendron* is cultivated for its ornamental value.[1] Various parts of these plants are used in traditional medicine. For example, leaves of *M. leucadendron* have been used for treating gout, respiratory ailments, inflammation, and dermatitis.[2,3] Additionally, the leaves of *Melaleuca alternifolia* have been used for treating psoriasis,[4] and the essential oil is used for skin and microbial infections.[5] The plant contains many phytochemicals such as hydrolyzable tannins,[6] polyphenols,[6] flavonoids,[7] triterpenes,[8,9] and stilbenes.[7] Some phytochemicals have exhibited various biological activities, such as antiviral,[10] antifungal,[11] anti-inflammatory,[12] antioxidant,[13] and antihistamine properties.[7]

Melaleuca quinquenervia (Cav.) S. T. Blake, commonly known as the "Cajeput tree", is an evergreen plant that is tough and adaptable. It is originally from Australia but has been introduced to many other parts of the world, including Hawai'i, where it is often used to protect against strong winds. The leaves of *M. quinquenervia* have been used in Thai folk medicine to treat microbial infections, gastrointestinal disorders, and skin lesions.[14] Previous phytochemical studies have identified flavanones, monoterpene glucosides, polyphenols with antioxidant potential, and compounds with antihyperglycemic activities in *M. quinquenervia*.[15,16] This report focuses on the bioassay-guided fractionation and structure elucidation of an ethyl acetate extract from *M. quinquenervia* fruits. The extract showed inhibitory effects on the growth of the A549 cell line

Received: January 26, 2024
Revised: March 22, 2024
Accepted: March 28, 2024
Published: April 11, 2024

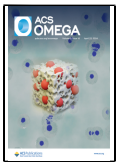

with an IC_{50} value of 35.8 ± 2.0 μg/mL, as demonstrated by the sulforhodamine B (SRB) cytotoxic assay.[29]

2. RESULTS AND DISCUSSION

Bioassay-guided fractionation of the ethyl acetate extract from *M. quinquenervia* fruits resulted in the isolation of two new flavanones (**1a** and **1b**), one new chalcone (**3**), along with 16 known compounds including (2*S*,11*R*) melanervin (**2a**),[17,18] (2*R*,11*S*) melanervin (**2b**),[17,18] pinocembrin (**4**),[19] strobopinin (**5**),[20] cryptostrobin (**6**),[21] *cis*-piceatannol (**7**),[22] piceatannol (**8**),[22] (1,1′-biphenyl)-2,2′,4,4′,5-pentol,3,3′,5′-trimethoxy (**9**),[23] 3,4,3′-tri-*O*-methylellagic acid (**10**),[24] 3-methoxy-5-methyl-1,2-benzenediol (**11**),[25] 2-methoxy-1,3,5-benzenetriol (**12**),[26] lupenone (**13**),[27] methyl betulinate (**14**),[28] 3-*O*-acetylbetulinic acid (**15**),[28] pyracrenic acid (**16**),[29] and oleanolic acid acetate (**17**).[30] The structures were determined by analyzing spectroscopic data such as UV, NMR, infrared (IR), and MS and comparing them to literature values.

Compound **1** was isolated as a colorless solid that gave an $[M + Na]^+$ ion at *m*/*z* 549.1506 in its HRESIMS spectrum, which corresponds to a molecular formula of $C_{31}H_{26}O_8$ with 19 degrees of unsaturation. The IR spectrum displayed the presence of hydroxy (3243 cm^{-1}), carbonyl (1613 cm^{-1}), and aromatic ring (1545, 1339, and 1258 cm^{-1}) functionalities. Analysis of its ^1H NMR spectral ($CDCl_3$, 400 MHz) data (Table 1) revealed the presence of a set of ABX-type protons [δ_H 5.46 (1H, dd, *J* = 12.0, 3.8 Hz, H-2), 2.97 (1H, dd, *J* = 17.1, 12.0 Hz, H-3α), 2.89 (1H, dd, *J* = 17.1, 3.8 Hz, H-3β)], one H-bonded hydroxy proton [δ_H 12.04 (1H, s, 5-OH)], two methyl singlets [δ_H 2.22 (3H, s, 6-CH_3), 1.49 (3H, s, 14-CH_3)], one methoxy proton [δ_H 3.90 (3H, s, 15-OCH_3)], one olefinic proton [δ_H 5.30 (1H, s, H-16)], one methine signal [δ_H 4.73 (1H, s, H-11)], and two sets of phenyl groups [δ_H 7.30 (4H, m, H-20/28), 7.28 (2H, m, H-21/27), 7.14 (2H, m, H-25/29), 7.07 (2H, m, H-19/23)]. The ^{13}C NMR spectrum ($CDCl_3$, 100 MHz) (Table 2) and HMQC correlations showed signals of 31 carbon signals that can be classified as three carbonyls (δ_C 196.6, 193.1, 164.7), 11 quaternary carbons (four sp^2 oxygenated carbons at δ_C 185.6,

Table 1. ^1H NMR (400 MHz) Spectroscopic Data of Compounds 1−3 (δ in ppm, *J* in Hz)

position	1[a]	2[a]	3[b]
2	5.46 (dd, 12.0, 3.8)	5.20 (dd, 13.2, 2.7)	7.78 (d, 16.0)
3	2.97 (dd, 17.1, 12.0), 2.89 (dd, 17.1, 3.8)	3.22 (dd, 17.1, 13.2), 2.84 (dd, 17.1, 2.7)	8.29 (d, 16.0)
11	4.73 (s)	6.21 (s)	
16	5.30 (s)	6.12 (s)	
19	7.07 (m)	7.33 (m)	
20	7.30 (m)	7.31 (m)	
21	7.28 (m)	7.35 (m)	
22	7.30 (m)	7.31 (m)	
23	7.07 (m)	7.33 (m)	
25	7.14 (m)	7.05 (m)	
26	7.30 (m)	7.13 (m)	
27	7.28 (m)	7.15 (m)	
28	7.30 (m)	7.13 (m)	
29	7.14 (m)	7.05 (m)	
2′			7.68 (m)
3′			7.44 (m)
4′			7.42 (m)
5′			7.44 (m)
6′			7.68 (m)
5″			6.12 (s)
5-OH	12.04 (s)	12.41 (s)	
6-CH_3	2.22 (s)	2.10 (s)	
14-CH_3	1.49 (s)	2.04 (s)	
15-OCH_3	3.90 (s)	3.76 (s)	
2″-OH			14.17 (s)
3″-CH_3			1.97 (s)
4″-OH			9.50 (br s)
6″-OH			10.12 (br s)

[a]Recorded in $CDCl_3$. [b]Recorded in acetone-d_6.

Table 2. ^{13}C NMR (100 MHz) Spectroscopic Data of Compounds 1−3 (δ in ppm)

position	1[a]	2[a]	3[b]
1			192.4
2	79.0	80.4	141.4
3	43.8	42.5	128.0
4	196.6	196.3	
5	159.9	161.0	
6	106.2	107.7	
7	154.8	162.9	
8	106.3	107.2	
9	155.5	156.2	
10	105.1	103.2	
11	42.2	35.1	
12	78.5	106.0	
13	164.7	152.5	
14	65.0	105.3	
15	185.6	158.0	
16	102.9	93.7	
17	193.1	152.9	
18	138.4	139.7	
19	128.5	128.8	
20	127.4	128.6	
21	128.8	129.4	
22	127.4	128.6	
23	128.5	128.8	
24	138.3	136.5	
25	125.4	126.7	
26	128.8	126.8	
27	127.6	126.3	
28	128.8	126.8	
29	125.4	126.7	
1′			135.8
2′			128.2
3′			128.9
4′			129.9
5′			128.9
6′			128.2
1″			104.6
2″			164.9
3″			102.8
4″			162.6
5″			94.4
6″			159.6
6-CH_3	7.3	7.7	
14-CH_3	24.6	8.3	
15-OCH_3	59.4	55.7	
3″-CH_3			6.6

[a]Recorded in $CDCl_3$. [b]Recorded in acetone-d_6.

https://doi.org/10.1021/acsomega.4c00769
ACS Omega 2024, 9, 18516−18525

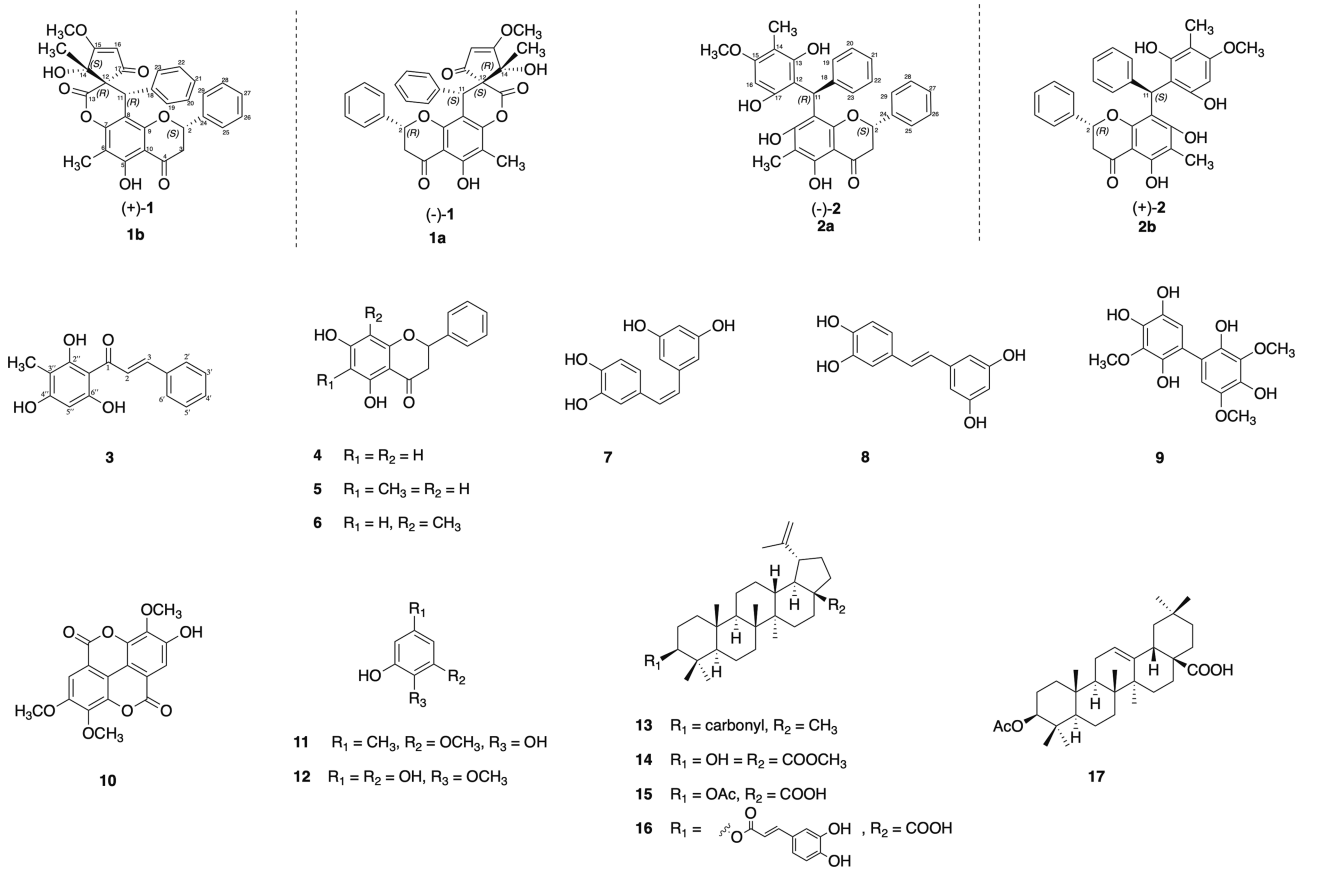

Figure 1. Structures of compounds **1**−**17** isolated from *M. quinquenervia* fruits.

159.9, 155.5, 154.8, five sp^2 carbons at δ_C 138.4, 138.3, 106.3, 106.2, 105.1, and two sp^3 carbons at δ_C 78.5, 65.0), 12 methines (one olefinic at δ_C 102.9 and two sp^3 at δ_C 79.0, 42.2), one methylene (δ_C 43.8), and three methyls (one sp^3 oxygenated at δ_C 59.4). The $^1H-^1H$ COSY correlations of H-2 through H_2-3, as well as the HMBC correlations (Figure 2) from H-2 (δ_H 5.46)

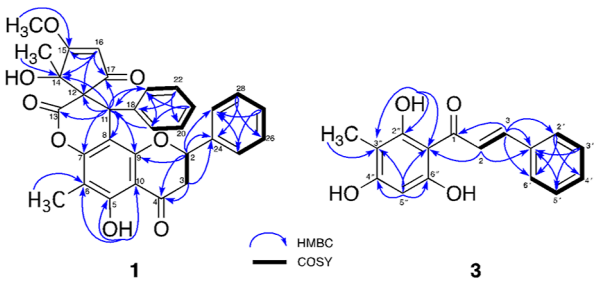

Figure 2. Key $^1H-^1H$ COSY and HMBC correlations of compounds **1** and **3**.

to C-3 (δ_C 43.8), C-4 (δ_C 196.6), C-9 (δ_C 155.5), and C-25/C-29 (δ_C 125.4); from 5-OH (δ_H 12.04) to C-5 (δ_C 159.9), C-6 (δ_C 106.2), and C-10 (δ_C 105.1); and from 6-CH_3 (δ_H 2.22) to C-5, C-6, and C-7 (δ_C 154.8), indicated the presence of a phenyl group and methyl group at C-2 (δ_C 79.0) and C-6, respectively. These signals resemble those of strobopinin,[20] a flavanone previously isolated from *Leptospermum scoparium*. A 4-hydroxy-3-methoxy-4-methylcyclopent-2-en-1-one moiety was constructed from the HMBC correlations from H-16 (δ_H 5.30) to C-12 (δ_C 78.5), C-14 (δ_C 65.0), C-15 (δ_C 185.6), and C-17 (δ_C 193.1); from 15-OCH_3 (δ_H 3.90) to C-15; and from 14-CH_3 (δ_H 1.49) to C-12, C-14, and C-15. Furthermore, the HMBC correlations from H-11 (δ_H 4.73) with C-7, C-8 (δ_C 106.3), C-9, C-12, C-13 (δ_C 164.7), C-14, C-17, and C-19/C-23 (δ_C 128.5) connected the other phenyl group and 4-hydroxy-3-methoxy-4-methylcyclopent-2-en-1-one subunit at C-11 and C-12, respectively. As mentioned above, these data accounted for 18 out of 19 degrees of unsaturation, requiring the presence of an additional ring. This finding implied that the oxygen and carbonyl groups at C-13 should be connected to form a δ-lactone. The relative configuration of **1** was established by the analysis of the NOESY data. The NOE correlations of H-11 to 14-CH_3 suggested that these protons were cofacial. The optical rotation of **1** was zero, and there were no Cotton effects in its electronic circular dichroism (ECD) spectrum, suggesting that **1** was a racemic mixture. Compound **1** was subjected to chiral-phase HPLC (Lux cellulose-1 column, Phenomenex) which afforded the two enantiomers (−)-**1** [t_R 13.8 min, $[\alpha]_D$ −19.6 (*c* 0.1, $CHCl_3$)] and (+)-**1** [t_R 16.9 min, $[\alpha]_D$ +20.2 (*c* 0.1, $CHCl_3$)]. A single crystal was obtained, and the structure of **1** was confirmed by single-crystal X-ray diffraction (Figure 3). The ECD curve of (+)-**1** (**1b**) showed positive Cotton effects at 257 and 232 nm, whereas (−)-**1** (**1a**) had opposite Cotton effects at the aforementioned wavelengths (Figure 4). Two putative structures of compound **1** (Figure 1) were optimized using the M06-2X/6-31+G* level in methanol and the ECD spectra for (2*S*,11*R*,12*R*,14*S*)-**1** and (2*R*,11*S*,12*S*,14*R*)-**1** were calculated at the M06-2X/def2-TZVPP level in methanol (Figure 5). Of these, the experimental ECD spectrum of (+)-**1** (**1b**) was similar to that of the computed ECD spectrum of (+)-(2*S*,11*R*,12*R*,14*S*)-**1** (Figure 5). Accordingly, the structures of compounds **1a** and **1b** were proposed as

https://doi.org/10.1021/acsomega.4c00769
ACS Omega 2024, 9, 18516−18525

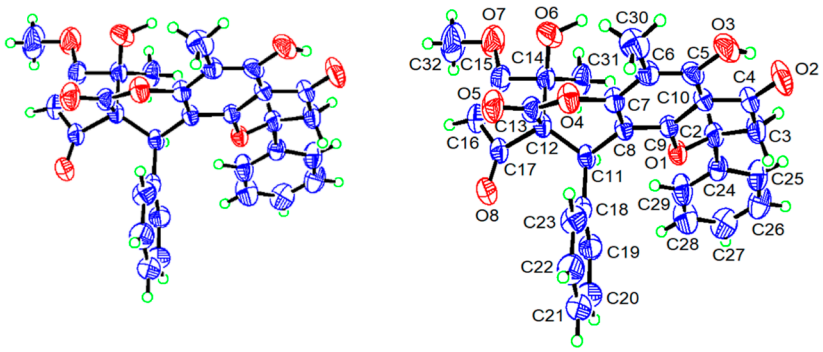

Figure 3. ORTEP drawings of spiroquinquenerin ($C_{31}H_{26}O_8 \cdot CH_3OH$); displacement ellipsoids are drawn at the 50% probability level at 298 K; methanol solvent molecule is not shown. Left: unlabeled and uncluttered view; right: labeled view.

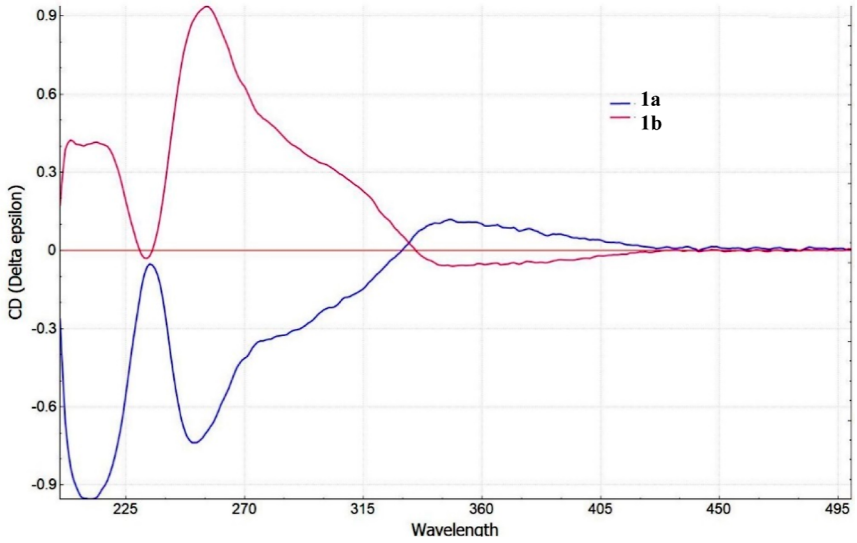

Figure 4. Experimental ECD spectra of **1a** and **1b**.

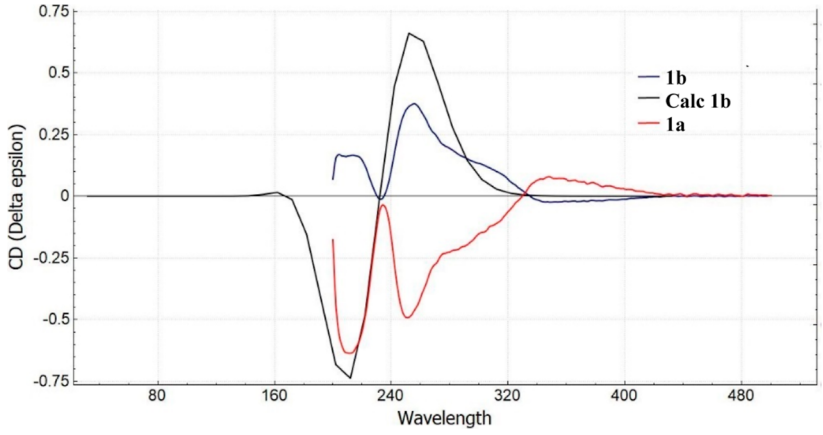

Figure 5. Calculated ECD spectra of **1**.

(−)-(2*R*,11*S*,12*S*,14*R*)-spiroquinquenerin (**1a**) and (+)-(2*S*,11*R*,12*R*,14*S*)-spiroquinquenerin (**1b**).

Compound **2** was initially obtained as a racemic mixture and was later separated into its pure enantiomers, **2a** and **2b**, using chiral-phase HPLC. The HRESIMS spectra of **2a** and **2b** gave an $[M + H]^+$ ion at m/z 513.1902 and 513.1910, respectively, indicating a molecular formula of $C_{31}H_{29}O_7$ (calcd for $C_{31}H_{29}O_7$, m/z 513.1913).[17,18] To determine the absolute configuration, we made a comparison between experimental and predicted ECD spectra. The experimental ECD curve for **2a** closely aligned with the predicted ECD curve of (2*S*,11*R*), exhibiting positive and negative Cotton effects at 230 and 300 nm, respectively. These findings support the absolute configurations of C-2 and C-11 being 2*S* and 11*R*, respectively. In contrast, **2b** displayed opposite Cotton effects at the same wavelengths (Figure S20).

Compound **3**, a dark yellow powder, gave the molecular formula $C_{16}H_{14}O_4$ from the molecular ion peak at m/z 271.0962

https://doi.org/10.1021/acsomega.4c00769
ACS Omega 2024, 9, 18516−18525

$[M + H]^+$ in the Q-TOFMS spectrum. The UV and IR spectra displayed the same pattern as those of chalcone core structures.[21] The ^{13}C NMR (acetone-d_6, 100 MHz) (Table 2) spectrum and HSQC correlations showed resonances of 16 carbon signals comprising one methyl, eight methines (two olefinics at δ_C 141.4, 128.0), and seven quaternary sp^2 carbons (one carbonyl at δ_C 192.4). In the ^1H and ^{13}C NMR spectra (Tables 1 and 2), the resonances for a *trans*-α,β-unsaturated ketone [δ_H 8.28 (1H, d, J = 16.0 Hz, H-3)/δ_C 128.0, 7.78 (1H, d, J = 16.0 Hz, H-2)/δ_C 141.4, and δ_C 192.4], a monosubstituted benzene ring [δ_H 7.68−7.42 (5H, m)], indicated that **3** has a chalcone skeleton. The location of the methyl group [δ_H 1.97 (3H, s)] at position 3 was deduced by HMBC correlations (Figure 2) from 2″-OH (δ_H 14.17) to C-1″ (δ_C 104.6), C-2″ (δ_C 164.9), and C-3″ (δ_C 102.8) and from 3″-CH_3 to C-2″, C-3″, and C-4′′ (δ_C 162.6). A singlet aromatic proton [δ_H 6.12 (1H, s)/δ_C 94.4] was determined to be located at C-5″ by the HMBC correlation of H-5″ with C-1″ and C-3′′. Furthermore, the HMBC spectrum exhibited interactions of H-3 (δ_H 8.28) with C-1′ (δ_C 135.8) and C-2′/C-6′ (δ_C 128.2) and correlation of H-2 with C-1′ and C-1″ confirming the attachment of a monosubstituted benzene ring at C-3. On the basis of these spectroscopic studies, the structure of **3** was defined as quinquenerin B.

Bioassay-guided fractionation was utilized to guide the chromatographic separation process. All fractions and isolated compounds, except for compound **1**, were evaluated for their cytotoxicity using a SRB assay in human nonsmall lung cancer A549 cells (Table 3). Cisplatin was used as a positive control and exhibited an IC_{50} value of 3.3 ± 0.0 μM in the A549 cells. Fractions C−F generated during chromatographic separation showed considerable cytotoxic activity. Their IC_{50} values ranged from 12.5 to 65.9 μg/mL. Among these fractions, C, D, E, and F showed noteworthy cytotoxicity toward the A549 cells, with IC_{50} values of 22.4, 17.1, 12.5, and 65.9 μg/mL, respectively. In contrast, fractions A and B were devoid of cytotoxicity, even at the highest concentration (100 μg/mL) tested (Figure 6). The isolated compounds (**2**, **14**, **15**, and **16**) were cytotoxic to nonsmall cell lung cancer (A549) cells with IC_{50} values of 13.5 ± 0.3, 11.0 ± 0.5, 11.0 ± 0.6, and 2.8 ± 0.1 μM, respectively (Table 3). Pyracrenic acid (**16**) was 2.6-fold more cytotoxic toward A549 lung cancer cells compared to nontumorigenic Vero E6 cells (selectivity index, SI = 2.6) (Figure 7). These results are encouraging, as pyracrenic acid (**16**) showed a level of selectivity similar to that of the chemotherapeutic drug cisplatin (SI = 3.0). In contrast, melanervin (**2**), methyl betulinate (**14**), and 3-*O*-acetylbetulinic acid (**15**) were almost equally cytotoxic toward A549 and Vero E6 (SI = 1.0−1.3). Pyracrenic acid (**16**), which is 3β-*O*-trans-caffeoylbetulinic acid, was found to be more cytotoxic toward A549 cells than 3-*O*-acetylbetulinic acid (**15**). These findings suggest that the isolated compounds have the potential to be developed further to improve their selectivity as lead compounds for anticancer drug discovery.[47]

Table 3. Cytotoxicity of Compounds 2−17 against A549 Cells Was Determined by an SRB Cytotoxicity Assay[a]

compounds	IC_{50} value (μM)
2	13.5 ± 0.3
2a	77.4 ± 2.9
2b	46.6 ± 1.1
3	131.1 ± 3.7
4	169.2 ± 2.1
5	285.8 ± 4.2
6	166.5 ± 2.0
7	215.7 ± 6.1
8	85.2 ± 4.0
9	97.0 ± 3.6
10	184.0 ± 3.9
11	IC_{50} > highest test concentration[b]
12	367.9 ± 10.2
13	IC_{50} > highest test concentration[b]
14	11.0 ± 0.5
15	11.1 ± 0.6
16	2.8 ± 0.1
17	143.3 ± 1.7
cisplatin	3.3 ± 0.0

[a]The IC_{50} values were calculated by treating the cells with isolated compounds or cisplatin for 72 h. The results of three independent experiments are shown as mean ± standard deviation values. [b]The IC_{50} value falls beyond the concentration range tested.

3. CONCLUSIONS

In conclusion, 19 compounds with varying structures were isolated from the fruits of *M. quinquenervia*. By analyzing the calculated and experimental CD data for compounds **1a**, **1b**, **2a**, and **2b**, we can determine the absolute configurations of enantiomers **1** and **2**, respectively. Due to insufficient sample quantity, compounds **1**, **1a**, and **1b** were not tested for cytotoxicity. It was noted that the naturally occurring racemate had a greater cytotoxic activity than each of the two pure isolated enantiomers of compound **2**. The two enantiomers might target different molecular pathways in A549 cells, resulting in a synergistic effect.

4. EXPERIMENTAL SECTION

4.1. General Experimental Procedures. Optical rotations were recorded in $CHCl_3$ on a Rudolph Research AUTOPOL IV multiwavelength polarimeter (Rudolph Research Analytical, Hackettstown, NJ, USA). Ultraviolet spectra were measured with a Shimadzu PharmaSpec-1800 UV−visible spectrophotometer (Shimadzu Scientific Instruments, Columbia, MD, USA). The ECD spectra were obtained on a JASCO J-815 spectropolarimeter (JASCO Inc., Tokyo, Japan). IR radiation spectra were measured on a Thermo Scientific Nicolet iS 10 FT-IR spectrometer (Thermo Fisher Scientific, Waltham, MA, USA). X-ray data were collected at 298 K using a Bruker D8 VENTURE four circle κ-geometry diffractometer equipped with an Incoatec IμS 3.0 microfocus sealed tube (Cu Kα radiation; λ = 1.54178 Å) with a multilayer mirror monochromator and a Photon III M14 area detector. NMR spectra, including bidimensional, were collected on a Bruker AVANCE DRX-400 NMR spectrometer (Bruker, Billerica, MA, USA) at 400 MHz (^1H) and 100 MHz (^{13}C), and the data were processed using MestReNova version 14.2.1-27684 software with $CDCl_3$ (δ_H 7.23, δ_C 77.16) or MeOD (δ_H 3.31, δ_C 49.0) as solvents. High-resolution electrospray ionization mass spectra were recorded on an Agilent 6530 LC-qTOF high mass accuracy mass spectrometer (Santa Clara, CA, USA) in positive ion mode. Silica gel (230−400 mesh, 480−800 mesh, Sorbent Technologies, Atlanta, GA, USA) and Sephadex LH-20 (GE Healthcare, Piscataway, NJ, USA) were used for column chromatography. Preparative HPLC was performed on a Thermo Scientific Ultimate 3000 system equipped with a

https://doi.org/10.1021/acsomega.4c00769
ACS Omega 2024, 9, 18516−18525

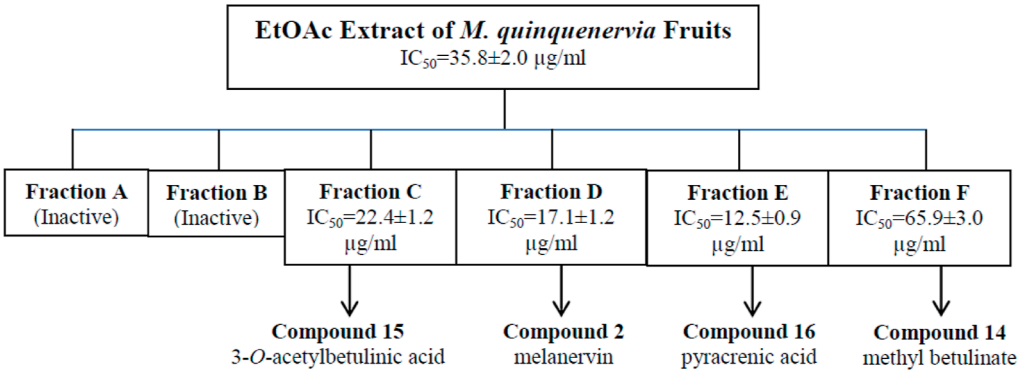

Figure 6. Cytotoxicity of *M. quinquenervia*: the EtOAc extract and chromatographic fractions were evaluated. Compounds **2**, **14**, **15**, and **16** had highly cytotoxic effects with lower IC_{50} values.

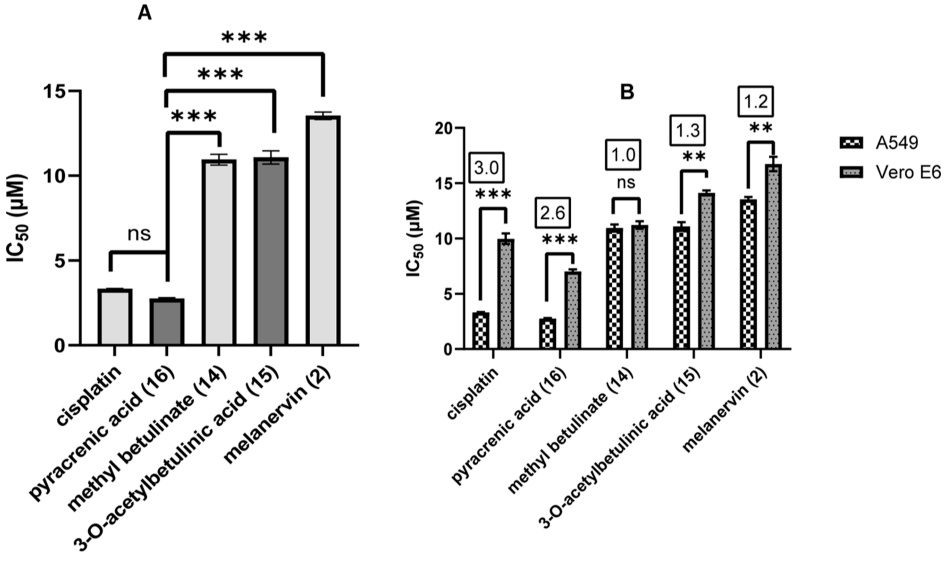

Figure 7. (A) IC_{50} values of compounds **2**, **14**, **15**, **16**, and cisplatin toward A549 cells. Data was obtained using a cytotoxicity assay based on the protein-binding dye, SRB. Cells were treated with increasing concentrations of test samples for 72 h. (B) The comparative cytotoxicity of compounds **2**, **14**, **15**, **16**, and cisplatin toward nonsmall cell lung cancer (A549) and Vero E6 (nontumorigenic) cells was analyzed. The SI values are shown in boxes above the bars. Results are shown as the mean ± standard deviation values of three independent experiments. ns = not significant, $^{*}p < 0.05$, $^{**}p < 0.01$, and $^{***}p < 0.001$ between two groups indicated.

photodiode array detector, using a reversed-phase C_{18} chiral column (250 × 10 mm, 5 μm, cellulose-1), with a flow rate of 2 mL/min.

4.2. Plant Material. The fresh fruits of *M. quinquenervia* were collected from Hilo, Hawai'i Island (Big Island), Hawaii, USA, in April 2022 and were identified by L. C. Chang. A voucher specimen (no. MQF01) was deposited at the Natural Product Chemistry Laboratory, Daniel K. Inouye College of Pharmacy, University of Hawai'i at Hilo.

4.3. Extraction and Isolation. The dried fruits of *M. quinquenervia* (1.4 kg) were extracted with EtOAc (3 L) at room temperature (3 days × thrice) and concentrated under reduced pressure to give an EtOAc extract (120.6 g). The extract was further separated by CC eluting with the gradient solvent systems of hexanes−EtOAc (1:0 to 0:1, v/v) and EtOAc−MeOH (1:0 to 0:1, v/v) to afford six fractions (A−F). Fractions C−F were active in the SRB cytotoxic assay (IC_{50} 17.7−65.9 μg/mL), while fractions A and B were inactive and were not investigated further. Fraction C (12.6 g) was washed with MeOH to yield **15** (1.7 g) and **17** (53.7 mg). Fraction D (6.2 g) was further separated by Sephadex LH-20 CC with 100% MeOH to afford four subfractions (Da−Dd). Purification of Dd (456.2 mg) by silica gel CC eluting with EtOAc−hexane (2:8, v/v) gave **4** (5.8 mg), **5** (12.8 mg), **2** (17.1 mg), and D1. Compound **2** was further purified by preparative chiral HPLC (acetonitrile−H_2O, 80:20, flow rate 2 mL/min) to furnish **2a** (t_R 20.3, 5.1 mg) and **2b** (t_R 22.1, 4.9 mg). Subfraction D1 (193.4 mg) was subjected to silica gel CC using EtOAc−DCM (1:49, v/v) to yield **1** (1.4 mg), **5** (6.6 mg), and **6** (9.3 mg). Compound **1** was further purified by preparative chiral HPLC (acetonitrile−H_2O, 60:40, flow rate 2 mL/min) to furnish **1a** (t_R 13.8, 0.4 mg) and **1b** (t_R 16.9, 0.3 mg). Fraction E (4.8 g) was purified by Sephadex LH-20 CC (100% MeOH) and followed by silica gel CC eluting with EtOAc−hexane (3:7, v/v) to **3** (2.1 mg), **9** (1.6 mg), **11** (11.3 mg), **13** (4.6 mg), and **16** (284.4 mg). Fraction F (6.1 g) was further purified on a Sephadex LH-20 CC (100% MeOH) and followed by silica gel CC eluting with MeOH−DCM (1:9, v/v) to yield **7** (8.2 mg), **8** (257.4 mg), **10** (2.7 mg), **12** (8.1 mg), and **14** (11.6 mg).

4.3.1. (−)-Spiroquinquenerin (1a). Colorless amorphous solid; UV (MeOH) λ_{max} (log ε): 220 (3.81), 274 (2.94) nm; CD (CH_3CN) λ_{max} ($\Delta\varepsilon$): 250 (−0.24), 225 (−0.018) nm; IR (neat) ν_{max}: 3246, 2962, 1613, 1545, 1262, 1018, 795 cm^{-1}; see Table 1 for ^1H NMR ($CDCl_3$, 400 MHz) and ^{13}C NMR ($CDCl_3$, 100

https://doi.org/10.1021/acsomega.4c00769
ACS Omega 2024, 9, 18516−18525

MHz); HRESIMS m/z: 549.1506 $[M + Na]^+$ (calcd for $C_{31}H_{26}NaO_8$, 549.1525).

*4.3.2. (+)-Spiroquinquenerin (**1b**).* Colorless amorphous solid; UV (MeOH) λ_{max} (log ε): 224 (3.87), 279 (3.25) nm; CD (CH_3CN) λ_{max} ($\Delta\varepsilon$): 257 (0.37), 232 (−0.01) nm; IR (neat) ν_{max}: 3243, 2948, 1607, 1551, 1258, 1012, 794 cm^{-1}; see Table 1 for ^1H NMR ($CDCl_3$, 400 MHz) and ^{13}C NMR ($CDCl_3$, 100 MHz); HRESIMS m/z: 549.1500 $[M + Na]^+$ (calcd for $C_{31}H_{26}NaO_8$, 549.1525).

*4.3.3. (2S,11R) Melanervin (**2a**).* Light yellow solid; mp 153−154 °C; see Table 1 for ^1H NMR ($CDCl_3$, 400 MHz) and ^{13}C NMR ($CDCl_3$, 100 MHz); HRESIMS m/z: 513.1902 $[M + H]^+$ (calcd for $C_{31}H_{29}O_7$, 513.1913).

*4.3.4. (2R,11S) Melanervin (**2b**).* Light yellow solid; mp 148−149 °C; see Table 1 for ^1H NMR ($CDCl_3$, 400 MHz) and ^{13}C NMR ($CDCl_3$, 100 MHz); HRESIMS m/z: 513.1910 $[M + H]^+$ (calcd for $C_{31}H_{29}O_7$, 513.1913).

*4.3.5. Quinquenerin B (**3**).* Dark yellow powder; mp 177−178 °C; UV (MeOH) λ_{max} (log ε): 240 (3.21), 275 (2.82) nm; IR (neat) ν_{max}: 3253, 1614, 1557, 1447, 1339, 1097, 972 cm^{-1}; see Table 1 for ^1H NMR (acetone-d_6, 400 MHz) and ^{13}C NMR (acetone-d_6, 100 MHz); HREIMS m/z: 271.0962 $[M + H]^+$ (calcd for $C_{16}H_{15}O_4$, 271.0970).

4.4. Cell Lines. A549 human lung carcinoma epithelial cells (CCL-185) and Vero E6 (CRL-1586, African green monkey kidney cells) were procured from the American Type Culture Collection (ATCC, Manassas, Virginia, USA). Cells were cultured in Dulbecco's modified Eagle's medium supplemented with heat-inactivated fetal bovine serum (FBS, 10%) and antibiotics (penicillin 1000 IU/mL and streptomycin 1000 μg/mL) at 37 °C in a humidified incubator with 5% CO_2.

4.5. SRB Cytotoxicity Assay. Cytotoxic activity was measured by an in vitro SRB assay as previously described.[31] A549 cells (6000 cells/well) or Vero E6 cells (8000 cells/well) were seeded in a 96-well plate for 24 h, followed by incubation for 72 h in the presence of test sample at increasing concentrations (1.25−50 μg/mL) or 0.5% DMSO (control). Cisplatin, at concentrations of 0.5−20 μM, was used as a positive control compound. After the incubation, cells were fixed with 50 μL of 10% trichloroacetic acid for 60 min at 4 °C. Next, the plate was washed repeatedly with water, dried, and stained with 100 μL of 0.4% SRB in 1% v/v acetic acid solution for 30 min. The plate was washed repeatedly with 1% acetic acid to remove the excess unbound dye and allowed to dry at room temperature. The protein-bound dye was solubilized in 200 μL of 10 mM Tris buffer (pH 10.0), and the optical density was recorded at 515 nm. Experiments were performed in triplicate. Percent cell death was calculated with the following equation

$$\%\ \text{Cell death} = \frac{(OD_C - OD_0) - (OD_S - OD_0)}{(OD_C - OD_0)} \times 100$$

OD_0 = optical density of cells before adding test sample/standard (0 day). This serves as the background reading. OD_C = optical density of cells in the control well at 72 h in the absence of test sample. OD_S = optical density of cells after 72 h of incubation with test sample/standard compound.

The median inhibitory concentration (IC_{50}) at which 50% cell death was observed was calculated by plotting % cell death against test sample concentration, after which nonlinear curve fit analysis was applied using the graphing and curve fitting software, GraphPad Prism. The SI was calculated using the following equation: SI = IC_{50} Vero E6 cells/IC_{50} A549 cells.[32−46]

4.6. Statistical Analysis. All data were presented as the mean ± standard error of the mean and were obtained from three separate experiments. Statistical analyses were performed by Student's t-test or ANOVA followed by Tukey's multiple comparisons test; $^*p < 0.05$, $^{**}p < 0.01$, and $^{***}p < 0.001$ denote statistical significance. IC_{50} values of A549 cells were calculated by nonlinear curve fit analysis using Prism software (GraphPad 10.0.2, San Diego, USA) with $R^2 > 0.9$ and $P > 0.5$ (runs test) as parameters of goodness of fit.

4.7. Computational Methods. For ECD prediction, conformers were searched using the experimental-torsion basic knowledge distance geometry (ETKDG)[48] conformer generator from RDkit with the Merck molecular force field.[49] Low-energy conformers within 5 kcal/mol of the lowest-energy conformer were then optimized in Gaussian 09[50] at the M06-2X[51]/6-31+G*[52] level with a polarizable continuum model[53] of methanol. Conformers were categorized into clusters based on their distance matrix deviations (DMD),[55] ignoring hydrogen and carbon atoms indistinguishable to rotation (for example, carbon atoms in the phenyl groups and hydrogen atoms in the methyl groups). Each cluster consisted of all conformers with DMD values within a threshold of 0.0015 Å, and these are considered as effectively the same species. Fifty-seven distinct clusters of conformers, verified by Visual Molecular Dynamics,[56] were identified and their electronic excitation energies and rotational strengths were calculated with time-dependent density functional theory[54] at the M06-2X/def2-TZVPP[52] level. The final ECD spectra were generated from the Boltzmann-weighted average of the 57 distinct conformer's ECD spectra using a sigma of 1/3099.6 nm^{-1} and were verified against the experimental spectrum of spiro-biflavonoid enantiomers (**1a** and **1b**).

4.8. Single-Crystal X-ray Structure Determination of Spiroquinquenerin (1). Crystals of spiroquinquenerin were obtained from methanol. A block-like specimen of approximate dimensions 0.05, 0.075, and 0.10 mm was mounted on a MiTeGen MicroMount. X-ray data were collected at 298 K using a Bruker D8 VENTURE four circle κ-geometry diffractometer equipped with an Incoatec IμS 3.0 microfocus sealed tube (Cu Kα radiation; λ = 1.54178 Å) with a multilayer mirror monochromator and a Photon III M14 area detector. A total of 2940 frames were collected and integrated with the Bruker SAINT software package by using a narrow-frame algorithm. The integration of the data using a triclinic unit cell yielded a total of 30,273 reflections to a maximum θ angle of 70.10° (0.82 Å resolution), of which 5117 were independent (average redundancy 5.92, completeness = 98.8%; R_{int} = 3.06%; R_{sig} = 2.01%). Data were corrected for absorption effects using the multiscan method (SADABS); T_{min} = 0.6928; T_{max} = 0.7533. The final unit cell constants are based upon the refinement of the XYZ-centroids of 9925 reflections above 20 σ(I) with 6.113 < 2θ < 140.1°. Crystal data for spiroquinquenerin: $C_{31}H_{26}O_8 \cdot CH_3OH$; M = 558.56; triclinic space group $P\bar{1}$; a = 9.5298(2) Å; b = 9.9515(2)(2) Å; c = 14.9005(3) Å; α = 94.6530(10)°; β = 102.4380(10)°; γ = 97.7540(10)°; V = 1358.42(5) Å^3; Z = 2 (Z' = 1); ρ = 1.366 g/cm^3; μ = 0.829 mm^{-1}; T = 298 K. The structure was solved using SHELXT, part of the Bruker software package APEX4; non-H atoms were refined anisotropically; H atoms were refined at idealized positions, riding on the neighboring atoms with relative isotropic displacement parameters. The final full-matrix least-squares refinement on

https://doi.org/10.1021/acsomega.4c00769
ACS Omega 2024, 9, 18516−18525

F^2 with 389 variables converged at R_1 = 5.45% for the observed data and wR_2 = 14.52% for all data; the goodness of fit (S) was 1.075. The final Fourier difference synthesis was featureless; the largest peak was 0.614 e/Å^3 (at a chemically implausible position) and the largest hole was −0.346 e/Å^3.

■ ASSOCIATED CONTENT

Supporting Information

The Supporting Information is available free of charge at https://pubs.acs.org/doi/10.1021/acsomega.4c00769.

Bioassay-guided isolation of *M. quinquenervia* fruit extract, ^{1}H NMR, ^{13}C NMR, COSY, HSQC, HMBC, and NOESY spectrum of compound **1**, HRESIMS spectrum of compound **1a** and **1b**, chiral HPLC chromatogram of **1a** and **1b**, ^{1}H NMR, ^{13}C NMR, COSY, HSQC, HMBC, and NOESY spectrum of compound **2**, HRESIMS spectrum of compound **2a** and **2b**, chiral HPLC chromatogram of **2a** and **2b**, experimental ECD spectra of **2a** and **2b**, calculated ECD spectra of **2**, ^{1}H NMR, ^{13}C NMR, COSY, HSQC, HMBC, and HRESIMS spectrum of compound **3**, Boltzmann distribution of conformers of **1b**, and XYZ coordinates of conformers of **1b** (PDF)

checkCIF/PLATON and crystal structure reports for compound **1** (PDF)

Crystallographic data for compound **1** (CIF)

Accession Codes

The supplementary crystallographic data for this paper can be found in the CCDC database under accession number 2239157. These data is available for free at www.ccdc.cam.ac.uk/data_request/cif, or by emailing data_request@ccdc.cam.ac.uk, or by contacting The Cambridge Crystallographic Data Centre, 12 Union Road, Cambridge CB2 1EZ, UK; fax: +44 1223 336033.

■ AUTHOR INFORMATION

Corresponding Author

Leng Chee Chang − *Department of Pharmaceutical Sciences, The Daniel K. Inouye College of Pharmacy, University of Hawai'i at Hilo, Hilo, Hawaii 96720, United States;* orcid.org/0000-0001-9918-5612; Phone: +1 (808) 932-8124; Email: lengchee@hawaii.edu; Fax: +1 (808) 933-2974

Authors

Achara Raksat − *Department of Pharmaceutical Sciences, The Daniel K. Inouye College of Pharmacy, University of Hawai'i at Hilo, Hilo, Hawaii 96720, United States*

Md Samiul Huq Atanu − *Department of Pharmaceutical Sciences, The Daniel K. Inouye College of Pharmacy, University of Hawai'i at Hilo, Hilo, Hawaii 96720, United States*

Sheyanne Mendez − *X-ray Diffraction Laboratory, Department of Chemistry, University of Hawai'i at Hilo, Hilo, Hawai'i 96720, United States*

Rafael de la Zerda − *Department of Chemistry, University of Hawai'i at Manoa, Honolulu, Hawaii 96822, United States*

Rui Sun − *Department of Chemistry, University of Hawai'i at Manoa, Honolulu, Hawaii 96822, United States;* orcid.org/0000-0003-0638-1353

Sarot Cheenpracha − *Division of Chemistry, School of Science, University of Phayao, Phayao 56000, Thailand;* orcid.org/0000-0002-4333-1059

Marisa Wall − *Daniel K. Inouye U.S. Pacific Basin Agricultural Research Center, Hilo, Hawaii 96720, United States*

Charles J. Simmons − *X-ray Diffraction Laboratory, Department of Chemistry, University of Hawai'i at Hilo, Hilo, Hawai'i 96720, United States*

Philip G. Williams − *Department of Chemistry, University of Hawai'i at Manoa, Honolulu, Hawaii 96822, United States;* orcid.org/0000-0001-8987-0683

Ghee T. Tan − *Department of Pharmaceutical Sciences, The Daniel K. Inouye College of Pharmacy, University of Hawai'i at Hilo, Hilo, Hawaii 96720, United States*

Supakit Wongwiwatthananukit − *Department of Pharmacy Practice, The Daniel K. Inouye College of Pharmacy, University of Hawai'i at Hilo, Hilo, Hawaii 96720, United States*

Complete contact information is available at: https://pubs.acs.org/10.1021/acsomega.4c00769

Notes

The authors declare no competing financial interest.

■ ACKNOWLEDGMENTS

This research was made possible by a cooperative agreement with the Agricultural Research Services, U.S. Department of Agriculture (no. NACA 58-2040-0-011) and the National Institute of Health, National Institute of General Medical Sciences (NIGMS), IDeA Networks of Biomedical Research Excellence (INBRE), award number: P20GM103466. C.J.S. acknowledges the National Science Foundation for their support in purchasing the Bruker D8 VENTURE X-ray diffractometer under grant no. 1919792. The content is solely the responsibility of the authors and does not necessarily represent the official views of the National Institutes of Health. We also acknowledge the Daniel K. Inouye College of Pharmacy for providing the mass spectrometry and NMR facility used in this research.

■ REFERENCES

(1) Southwell, I. A.; Russell, M. F. Volatile oil comparison of cotyledon leaves of chemotypes of *Melaleuca alternifolia*. *Phytochemistry* **2002**, *59*, 391−393.

(2) Nguyen, M. T.; Awale, S.; Tezuka, Y.; Tran, Q. L.; Watanabe, H.; Kadota, S. Xanthine oxidase inhibitory activity of Vietnamese medicinal plants. *Biol. Pharm. Bull.* **2004**, *27*, 1414−1421.

(3) Niang, S. O.; Tine, Y.; Diatta, B. A.; Diallo, M.; Fall, M.; Seck, N. B.; Kane, A. Negative cutaneous effects of medicinal plants in Senegal. *Br. J. Dermatol.* **2015**, *173*, 26−29.

(4) Amenta, R.; Camarda, L.; Di Stefano, V.; Lentini, F.; Venza, F. Traditional medicine as a source of new therapeutic agents against psoriasis. *Fitoterapia* **2000**, *71*, S13−S20.

(5) Camp, R. D. The Wizard of Oz,11Australia, commonly referred to by Australians and the British as "Oz". or the Intriguing Tale of the Tea Tree. *J. Invest. Dermatol.* **2004**, *123*, xviii−xvxix.

(6) Yoshida, T.; Maruyama, T.; Nitta, A.; Okuda, T. An hydrolysable tannin and accompanying polyphenols from *Melaleuca leucadendron*. *Phytochemistry* **1996**, *42*, 1171−1173.

(7) Tsuruga, T.; Chun, Y. T.; Ebizuka, Y.; Sankawa, U. Biologically active constituents of *Melaleuca leucadendron*: inhibitors of induced histamine release from rat mast cells. *Chem. Pharm. Bull.* **1991**, *39*, 3276−3278.

(8) Lee, C. K. A new norlupene from the leaves of *Melaleuca leucadendron*. *J. Nat. Prod.* **1998**, *61*, 375−376.

(9) Lee, C. K.; Chang, M. H. Four new triterpenes from the heartwood of *Melaleuca leucadendron*. *J. Nat. Prod.* **1999**, *62*, 1003−1005.

(10) Nawawi, A. A.; Nakamura, N.; Hattori, M.; Kurokawa, M.; Shiraki, K. Inhibitory effects of Indonesian medicinal plants on the infection of herpes simplex virus type 1. *Phytother Res.* **1999**, *13*, 37−41.

(11) Zhang, J.; Wu, H.; Jiang, D.; Yang, Y.; Tang, W.; Xu, K. The antifungal activity of essential oil from *Melaleuca leucadendra* (L.) L.

grown in China and its synergistic effects with conventional antibiotics against Candida. *Nat. Prod. Res.* **2019**, *33*, 2545−2548.
(12) Al-Sayed, E.; Korinek, M.; Esmat, A.; Chen, G. Y.; Cheng, Y. B.; Hsieh, P. W.; Chen, B. H.; Hwang, T. L. Anti-inflammatory, hepatoprotective and antioxidant activity of ellagitannin isolated from *Melaleuca styphelioides*. *Phytochemistry* **2020**, *177*, 112429.
(13) Seligmann, O.; Wagner, H. Structure determination of melanervin, the first naturally occurring flavonoid of the triphenylmethane family. *Tetrahedron* **1981**, *37*, 2601−2606.
(14) Sharifi-Rad, J.; Salehi, B.; Varoni, E. M.; Sharopov, F.; Yousaf, Z.; Ayatollahi, S. A.; Kobarfard, F.; Sharifi-Rad, M.; Afdjei, M. H.; Sharifi-Rad, M.; Iriti, M. Plants of the *Melaleuca* genus as antimicrobial agents: from farm to pharmacy. *Phytother Res.* **2017**, *31*, 1475−1494.
(15) Moharram, F. A.; Marzouk, M. S.; El-Toumy, S. A. A.; Ahmed, A. A. E.; Aboutabl, E. A. Polyphenols of *Melaleuca quinquenervia* leaves - pharmacological studies of grandinin. *Phytother Res.* **2003**, *17*, 767−773.
(16) Aboutabl, E. A.; Soliman, H. S. M.; Moharram, F. A. Melacoside A, a novel monoterpene glucoside from *Melaleuca quinquenervia* (Cav.) S.T. Blake. *Al-Azhar J. Pharm. Sci.* **1999**, *23*, 110−115.
(17) Matsuura, S. The structure of cryptostrobin and strobopinin, the flavanones from the heartwood of *Pinus strobus*. *Pharm. Bull.* **1957**, *5* (3), 195−198.
(18) Seligmann, O.; Wagner, H. Structure determination of melanervin, the first naturally occurring flavonoid of the triphenylmethane family. *Tetrahedron* **1981**, *37* (15), 2601−2606.
(19) Bick, I. C.; Brown, R.; Hillis, W. Three flavanones from leaves of *Eucalyptus sieberi*. *Aust. J. Chem.* **1972**, *25*, 449−451.
(20) Mayer, R. Flavonoids from *Leptospermum scoparium*. *Phytochemistry* **1990**, *29*, 1340−1342.
(21) Cannon, J. R.; Martin, P. F. The flavanones of *Agonis spathulata* (myrtaceae). *Aust. J. Chem.* **1977**, *30*, 2099−2101.
(22) Piano, F.; Bertolone, E.; Pes, D.; Asproudi, A.; Borsa, D. Focusing on bioactive compounds in grapes: stilbenes in *Uvalino* cv. *Eur. Food Res. Technol.* **2013**, *237*, 897−904.
(23) Yu, L.; Smith, J.; Laskin, A.; George, K. M.; Anastasio, C.; Laskin, J.; Dillner, A. M.; Zhang, Q. Molecular transformations of phenolic SOA during photochemical aging in the aqueous phase: competition among oligomerization, functionalization, and fragmentation. *Atmos. Chem. Phys.* **2016**, *16*, 4511−4527.
(24) Dellagreca, M.; Fiorentino, A.; Monaco, P.; Previtera, L.; Sorrentino, M. Antialgal phenylpropane glycerides from *Juncus effusus*. *Nat. Prod. Lett.* **1998**, *12*, 263−270.
(25) Choomuenwai, V.; Beattie, K. D.; Healy, P. C.; Andrews, K. T.; Fechner, N.; Davis, R. A. Entonalactams A-C: Isoindolinone derivatives from an Australian rainforest fungus belonging to the genus Entonaema. *Phytochemistry* **2015**, *117*, 10−16.
(26) Xiao, Z. P.; Shi, D. H.; Li, H. Q.; Zhang, L. N.; Xu, C.; Zhu, H. L. Polyphenols based on isoflavones as inhibitors of *Helicobacter pylori* urease. *Bioorg. Med. Chem.* **2007**, *15*, 3703−3710.
(27) Tinto, W. F.; Blair, L. C.; Alli, A.; Reynolds, W. F.; McLean, S. Lupane triterpenoids of *Salacia cordata*. *J. Nat. Prod.* **1992**, *55*, 395−398.
(28) Macías, F. A.; Simonet, A. M.; Esteban, M. D. Potential allelopathic lupane triterpenes from bioactive fractions of *Melilotus messanensis*. *Phytochemistry* **1994**, *36*, 1369−1379.
(29) Chen, B.; Duan, H.; Takaishi, Y. Triterpene caffeoyl esters and diterpenes from *Celastrus stephanotifolius*. *Phytochemistry* **1999**, *51*, 683−687.
(30) Alves, H. M.; Arndt, V. H.; Ollis, W. D.; Eyton, W. B.; Gottlieb, O. R.; Magalhães, M. Triterpenoids isolated from *Machaerium incorruptibile*. *Phytochemistry* **1966**, *5*, 1327−1330.
(31) Han, C.; Raksat, A.; Atanu, M. S. H.; Chang, L. K.; Wall, M. M.; Chang, L. C. Investigation of antimicrobial, antioxidant, and cytotoxic activities of *Boesenbergia rotunda* rhizome extract. *J. Curr. Sci. Technol.* **2024**, *14* (1), 20.
(32) Li, Z. Q.; Scheraga, H. A. Monte Carlo-minimization approach to the multiple-minima problem in protein folding. *Proc. Natl. Acad. Sci. U.S.A.* **1987**, *84*, 6611−6615.
(33) Kaminski, G. A.; Friesner, R. A.; Tirado-Rives, J.; Jorgensen, W. L. Evaluation and reparametrization of the OPLS-AA force field for proteins via comparison with accurate quantum chemical calculations on peptides. *J. Phys. Chem. B* **2001**, *105*, 6474−6487.
(34) *Schrödinger Release 2020-4: MacroModel Software*; Schrödinger LLC: New York, NY, 2020.
(35) Frisch, M. J.; Trucks, G. W.; Schlegel, H. B.; Scuseria, G. E.; Robb, M. A.; Cheeseman, J. R.; Scalmani, G.; Barone, V.; Mennucci, B.; Petersson, G. A.; Nakatsuji, H.; Caricato, M.; Li, X.; Hratchian, H. P.; Izmaylov, A. F.; Bloino, J.; Zheng, G.; Sonnenberg, J. L.; Hada, M.; Ehara, M.; Toyota, K.; Fukuda, R.; Hasegawa, J.; Ishida, M.; Nakajima, T.; Honda, Y.; Kitao, O.; Nakai, H.; Vreven, T.; Montgomery, J. A.; Peralta, J. E.; Ogliaro, F.; Bearpark, M.; Heyd, J. J.; Brothers, E.; Kudin, K. N.; Staroverov, V. N.; Kobayashi, R.; Normand, J.; Raghavachari, K.; Rendell, A.; Burant, J. C.; Iyengar, S. S.; Tomasi, J.; Cossi, M.; Rega, N.; Millam, J. M.; Klene, M.; Knox, J. E.; Cross, J. B.; Bakken, V.; Adamo, C.; Jaramillo, J.; Gomperts, R.; Stratmann, R. E.; Yazyev, O.; Austin, A. J.; Cammi, R.; Pomelli, C.; Ochterski, J. W.; Martin, R. L.; Morokuma, K.; Zakrzewski, V. G.; Voth, G. A. S. P.; Dannenberg, J. J.; Dapprich, S.; Daniels, A. D.; Farkas; Foresman, J. B.; Ortiz, J. V. C. J.; Fox, D. J. *Gaussian 09*; Gaussian Inc., 2009.
(36) Yanai, T.; Tew, D. P.; Handy, N. C. A new hybrid exchange-correlation functional using the Coulomb-attenuating method (CAM-B3LYP). *Chem. Phys. Lett.* **2004**, *393*, 51−57.
(37) Clark, T.; Chandrasekhar, J.; Spitznagel, G. W.; Schleyer, P. V. R. Efficient diffuse function-augmented basis sets for anion calculations. III. The 3-21+G basis set for first-row elements, Li-F. *J. Comput. Chem.* **1983**, *4*, 294−301.
(38) Ditchfield, R.; Hehre, W. J.; Pople, J. A. Self-consistent molecular-orbital methods. IX. An extended Gaussian-type basis for molecular-orbital studies of organic molecules. *J. Chem. Phys.* **1971**, *54*, 724−728.
(39) Hehre, W. J.; Ditchfield, R.; Pople, J. A. Self—consistent molecular orbital methods. XII. further extensions of Gaussian—type basis sets for use in molecular orbital studies of organic molecules. *J. Chem. Phys.* **1972**, *56*, 2257−2261.
(40) Hariharan, P. C.; Pople, J. A. The influence of polarization functions on molecular orbital hydrogenation energies. *Theor. Chim. Acta* **1973**, *28*, 213−222.
(41) Tomasi, J.; Mennucci, B.; Cammi, R. Quantum mechanical continuum solvation models. *Chem. Rev.* **2005**, *105*, 2999−3094.
(42) Runge, E.; Gross, E. K. U. Density-functional theory for time-dependent systems. *Phys. Rev. Lett.* **1984**, *52*, 997−1000.
(43) Gross, E. K. U.; Dobson, J. F.; Petersilka, M. Density functional theory of time-dependent phenomena. *Top. Curr. Chem.* **1996**, *181*, 81−172.
(44) Grauso, L.; Teta, R.; Esposito, G.; Menna, M.; Mangoni, A. Computational prediction of chiroptical properties in structure elucidation of natural products. *Nat. Prod. Rep.* **2019**, *36*, 1005−1030.
(45) Bruhn, T.; Schaumlöffel, A.; Hemberger, Y.; Pescitelli, G. *Spec Disversion 1.71*; University of Pisa: Berlin, Germany, 2017. Available at: http:/specdis-software.jimdo.com.
(46) Lu, T.; Chen, F. Multiwfn: a multifunctional wavefunction analyzer. *J. Comput. Chem.* **2012**, *33*, 580−592.
(47) Kim, D. J.; Kang, Y. H.; Kim, K. K.; Kim, T. W.; Park, J. B.; Choe, M. Increased glucose metabolism and alpha-glucosidase inhibition in *Cordyceps militaris* water extract-treated HepG2 cells. *Nutr. Res. Prac.* **2017**, *11*, 180−189.
(48) Riniker, S.; Landrum, G. A. Better informed distance geometry: using what we know to improve conformation generation. *J. Chem. Inf. Model.* **2015**, *55*, 2562−2574.
(49) Halgren, T. A. Merck molecular force field. I. Basis, form, scope, parameterization, and performance of MMFF94. *J. Comput. Chem.* **1996**, *17*, 490−519.
(50) Frisch, M. J.; Trucks, G. W.; Schlegel, H. B.; Scuseria, G. E.; Robb, M. A.; Cheeseman, J. R.; Scalmani, G.; Barone, V.; Mennucci, B.; Petersson, G. A.; et al. *Gaussian 09*, Revision, B.01; Gaussian Inc.: Wallingford, CT, USA, 2009.

https://doi.org/10.1021/acsomega.4c00769
ACS Omega 2024, 9, 18516−18525

(51) Hohenstein, E. G.; Chill, S. T.; Sherrill, C. D. Assessment of the performance of the M05- 2X and M06-2X exchange-correlation functionals for noncovalent interactions in biomolecules. *J. Chem. Theory Comput.* **2008**, *4*, 1996−2000.
(52) Pritchard, B. P.; Altarawy, D.; Didier, B.; Gibson, T. D.; Windus, T. L. New basis set exchange: an open, up-to-date resource for the molecular sciences community. *J. Chem. Inf. Model.* **2019**, *59*, 4814−4820.
(53) Tomasi, J.; Mennucci, B.; Cammi, R. Quantum mechanical continuum solvation models. *Chem. Rev.* **2005**, *105*, 2999−3094.
(54) Runge, E.; Gross, E. Density-functional theory for time-dependent systems. *Phys. Rev. Lett.* **1984**, *52*, 997−1000.
(55) Lesk, A. M. Extraction of well-fitting substructures: root-mean-square deviation and the difference distance matrix. *Folding Des.* **1997**, *2*, S12−S14.
(56) Humphrey, W.; Dalke, A.; Schulten, K. VMD: Visual molecular dynamics. *J. Mol. Graph.* **1996**, *14*, 33−38.

https://doi.org/10.1021/acsomega.4c00769
ACS Omega 2024, 9, 18516−18525